Pertanika J. Sci. & Technol. 32 (6): 2421 - 2440 (2024)

PERTANIKA JOURNALS

SCIENCE & TECHNOLOGY

Journal homepage: http://www.pertanika.upm.edu.my/

Bernoulli Distillation System (BDS) for Bioethanol Sorghum Stalk Purification

Djoko Wahyudi[1]*, Wignyanto[2], Yusuf Hendrawan[3] and Nurkholis Hamidi[4]

[1]Department of Mechanical Engineering, Faculty of Engineering and Informatics, Panca Marga Unuversity, Yos Sudarso 107 Dringu, Probolinggo, East Java, Indonesia
[2]Department of Agro Industry Engineering, Faculty of Agricultural Technology, Brawijaya University, Veteran St, Malang, East Java, ZIP 65145, Indonesia
[3]Department of Biosystem Engineering, Faculty of Agricultural Technology, Brawijaya University, Veteran St, Malang, East Java, ZIP 65145, Indonesia
[4]Department of Mechanical Engineering, Faculty of Engineering, Brawijaya University, Veteran St, Malang, East Java, ZIP 65145, Indonesia

ABSTRACT

Sorghum is a plant that produces syrup, forage and animal feed silage. The utilization of sorghum stalk as fuel oil (bioethanol) is an energy increasingly needed by the depletion of deposits of fossil fuel oil. Thus, tools and methods are needed to produce sorghum stem bioethanol, which has a certain purity level. This study aims to increase the purity of bioethanol from sorghum stems using the Bernoulli Distillation System (BDS) by experimentally testing the purification of sorghum stem bioethanol. In the bioethanol purification stage, heat transfer in the reactor and condenser was analyzed, and the performance of the ejector was analyzed with a vacuum pressure (-55 cmHg), temperature 71°C, test time of 1800, 3600, 5400 and 7200 seconds with a test material of 28% capacity 20 liters. The results of the analysis of the highest conduction heat transfer on the water jacket wall are 14757.72 Joules, the reactor tank is 962.1 Joules, the bottom of the reactor tank is 765.05 Joules and convection in the reactor fluid is 2.09 Joules. The highest heat transfer energy in the condenser is 72683.1 Joules. While the efficiency of the water jet ejector is 65.4%, the highest increase in bioethanol content is 51% in 3600 seconds, as much as 745 ml. The characteristics of the bioethanol obtained included a calorific value test of 1389.48 cal/gram, a viscosity of 1.02044, a flash point of 32.5°C, and a

ARTICLE INFO

Article history:
Received: 03 September 2023
Accepted: 12 April 2024
Published: 09 October 2024

DOI: https://doi.org/10.47836/pjst.32.6.02

E-mail addresses:
djokowahyudi@gmail.com (Djoko Wahyudi)
wignyanto@ub.ac.id (Wignyanto)
yusufhendrawan@gmail.com (Yusuf Hendrawan)
hamidi@ub.ac.id (Nurkholis Hamidi)
* Corresponding author

ISSN: 0128-7680
e-ISSN: 2231-8526

density of 0.934 g/cm^3. Thus, the Bernoulli Distillation System's purification process can increase bioethanol levels effectively and efficiently.

Keywords: Bioethanol purification, heat transfer energy, sorghum stalk

INTRODUCTION

Bioethanol is a type of alternative energy that can be used in engines as a source of heat energy. Bioethanol raw materials can be obtained from plants. One of the plants that has the potential to be processed into bioethanol is sorghum (Malherbe et al., 2023). In Indonesia, sorghum can be found on Java, Kalimantan, Sulawesi, and Nusa Tenggara islands. Sorghum contains relatively high glucose and has a much higher biomass production when compared to sugar cane (Ndapamuri et al., 2021). If viewed from the harvest cycle, sorghum can be harvested earlier than sugarcane. The harvest cycle of sorghum is around 4 months, while that of sugar cane is 7 months. In terms of physical properties, sorghum has a glucose content of 11%–16% and 10%–14.4% sucrose, while sugarcane contains 10%–18% and 9%–17% sucrose. The glucose content is quite high in sorghum, so sorghum has the potential to be developed as a bioethanol product (Suryaningsih & Irhas, 2014).

Processing is required to convert sorghum into bioethanol. Generally, sorghum processing into bioethanol can be carried out through separation and purification (Kartawiria et al., 2015). It is done to produce optimal bioethanol products. The optimal product can be seen from the resulting bioethanol product's yield and physical and chemical properties (Nnaemeka et al., 2021). Separating and purifying raw materials into bioethanol is carried out during the distillation stage (Chen & Fu, 2016). However, the distillation stage requires concrete and renewable innovation because the bioethanol products are still average and have low alcohol content, causing high production costs. Therefore, it is necessary to research the bioethanol production process. Bioethanol production is still being done using a simple distillation system. The simple distillation process produces bioethanol products that are low in yield and alcohol content. Therefore, further research is needed to increase the yield and alcohol content. One way that can be done is by using a vacuum distillation system.

Vacuum distillation has the advantage of being able to separate two or more fluid components based on differences in their boiling points (Luyben, 2022). The boiling liquid converts to vapor. Steam is flowed into the condensate to be cold-treated so that it becomes a liquid fluid. However, liquid fluids that have lower boiling points will evaporate first. The boiling point of pure ethanol is 78°C, and water's is 100°C (standard conditions). At 78°C, ethanol evaporates first, followed by water. Vacuum distillation reduces the air pressure in the distillation so that the boiling point of the separated compounds is lower than the boiling point at normal atmospheric pressure (Benedetto et al., 2018; Sippola & Taskinen, 2018). Thus, these compounds can be separated more easily. Bioethanol production is processed using vacuum distillation using a vacuum system reactor. A vacuum distillation reactor functions

to convert xylose compounds or glucose into bioethanol (Aditiya et al., 2016). However, the vacuum distillation process cannot be separated from the heat transfer scheme. Heat transfer in the reactor will determine the resulting bioethanol product (Almeida et al., 2021). Heat transfer is a form of energy transfer that moves from a system to the environment or the surrounding system. So, heat can move across the boundary of one system to another. Heat transfer occurs due to the difference in temperature between the system and its surroundings (Jiaqiang et al., 2018). Research is needed on the heat rate that has reacted with the material used to determine the heat transfer. Two factors, namely the material and the rate of heat transfer, determine the resulting bioethanol product (Zabed et al., 2017).

Quality bioethanol can be produced through the right process by calculating convection heat transfer. Proper thermal energy is needed to convert glucose into bioethanol products (Chandan et al., 2022). If the thermal treatment is less than or exceeds the limit, it will change the structure of glucose so that the resulting bioethanol product does not comply with established standards. Changing the glucose structure damages the carbon chains, so the resulting calorific value becomes low. The heat transfer rate can be calculated by calculating the total heat transfer in the surface area subject to heat (Allan et al., 2022). Data on the temperature of the incoming and outgoing fluids, the total heat transfer coefficient, the total heat transfer rate, and other supporting data are needed to obtain data on the total heat transfer rate. This data can be known by calculating the energy balance between hot and cold fluids, ignoring heat transfer that occurs to the environment and changes in kinetic and potential energy.

Similar research was conducted by Li et al. (2023). The research examined optimizing heat transfer and temperature control of battery thermal management systems based on composite phase change materials. The results of the study stated that if two objects with different temperatures are placed in contact with each other, heat will flow from the object with a higher temperature to the object with a lower temperature. This instantaneous heat transfer is always in the direction that tends to equalize the temperature. If this is allowed, the temperatures of the two will be the same, and both are said to be in a state of thermal equilibrium, meaning no heat transfer occurs between the two.

Xiao et al. (2023), in their research entitled "Effects of circumferential heat conduction on heat transfer characteristics of supercritical R134a in horizontal tubes," simulated supercritical heat transfer of R134a in horizontal tubes in order to study the effect of circular heat conduction on heat transfer damage, and the phenomenon of abnormal temperature distribution that is higher than the flow non-gravitational supercritical is described. The results show that heat transfer deterioration is due to specific heat disturbance and heat conduction in the boundary layer. In contrast, heat transfer is due to increased thermal conduction and turbulent convection after recovery. A dimensionless parameter Biot number is defined to characterize the thermal resistance ratio of a differential conductive environment to convective heat transfer. The redistribution of wall temperature due to

conduction entails circumferential influences supercritical convection in the horizontal tube. Non-gravitational supercritical flow may have higher wall temperatures when the Bi number is small. Top surface damage can be significantly reduced in tubes with greater wall thickness or thermal conductivity.

Murshed presents a cutting-edge review of the research and development of the conduction (thermal conductivity) and convection heat transfer characteristics of ethylene glycol-based nanofluids. Methods of preparation and stabilization of nanofluids are summarized and discussed. The effects of nanoparticle type, size and concentration, as well as temperature, on the thermal conductivity of nanofluids based on available ethylene glycol and ethylene glycol/water mixtures have been analyzed and discussed critically and individually. Studies on convective heat transfer of these nanofluids have also been reviewed, and results from different studies have been compared. The review clearly shows that this nanofluid has much higher thermal conductivity and convective heat transfer characteristics compared to its base fluid, i.e., ethylene glycol and aqueous mixtures. The thermal features of these nanofluids are a key factor for their performance in thermal management and energy applications. With their enhanced thermal conductivity and convective heat transfer coefficient, nanofluids offer great potential in energy harvesting and storage as well as for advanced cooling applications (Murshed & Castro, 2016).

Effendy et al. (2013) conducted a study entitled "Effect of mesh topologies on wall heat transfer and pressure loss prediction of a blade coolant passage." The results showed that the manufacture of grid mesh greatly influenced the heat transfer coefficient and pressure loss. In addition, according to Manente et al. (2022), wasted heat energy can be reduced by placing heat insulation around the reactor.

Gholinia et al. (2018) researched the water jacket to find the temperature on the water jacket wall. The results showed that the temperature of the water jacket along the height of the combustion chamber wall increased until it reached its boiling point. However, the temperature gradient decreases when the water jacket flow is higher. Further research is necessary based on the description above and the research done. This study analyzes the heat transfer energy in the reactor and condenser and the effectiveness of the ejector in bioethanol purification to increase bioethanol content. Further research was conducted to optimize the production of bioethanol from sorghum stems. The research was carried out using thermal energy transfer testing. The research results analyze the thermal energy in the reactor and condenser. This study will discuss and analyze the scope of the research, including the reactor's and condenser's thermal energy for sorghum stalk bioethanol purification with a vacuum distillation system. The vacuum distillation system is used by applying the Bernoulli system so that the vacuum process does not use a vacuum pump. Thus, the tool designed is named the Bernoulli Distillation System (BDS). Applying the Bernoulli system in the form of a water ejector makes the bioethanol purification process maximally efficient and produces an increasing number of purified bioethanol products.

MATERIALS AND METHODS

The material used during the test was sorghum stalk bioethanol. However, before becoming bioethanol, treatment is required so that it goes through a fermentation process. The process of processing sorghum into bioethanol begins with the selection of quality sorghum materials. Quality sorghum is selected so that the resulting sap is optimal. Sorghum is pressed on the stem using a sugar press. The process of taking sorghum sap is shown in Figure 1. The result of pressing is sorghum sap. Then, the sorghum sap is continued with the fermentation process. The treatment used in this process is the Batch system.

Figure 1. A taking of sorghum stalk nira

Making sorghum bioethanol begins with heating the nira at 40°C for 10 minutes. After the heating process, Saccharomyces cerevisiae (yeast), NPK (Nitrogen, Phosphorus and Kalium), and Urea were added. Saccharomyces cerevisiae was added to 2% of the total mass of nira (m/m), 0.5% NPK (m/m), and 0.2% urea (m/m). Then, after adding it, it was stirred until evenly distributed. The nira and the mixture are placed in a container and fermented for seven days. In the fermentation process, carbohydrate feed was added so that the microbes grow and develop. After seven days, the distillation process is continued at 70°C. The resulting bioethanol product will be measured for its bioethanol content using an alcohol meter so that the value of the bioethanol content is known before the purification process is carried out. Figure 2 shows the scheme for making sorghum bioethanol.

The design of the bioethanol purification process tool in this study is one of the most important parts (Amornraksa et al., 2020). Success in testing is highly dependent on

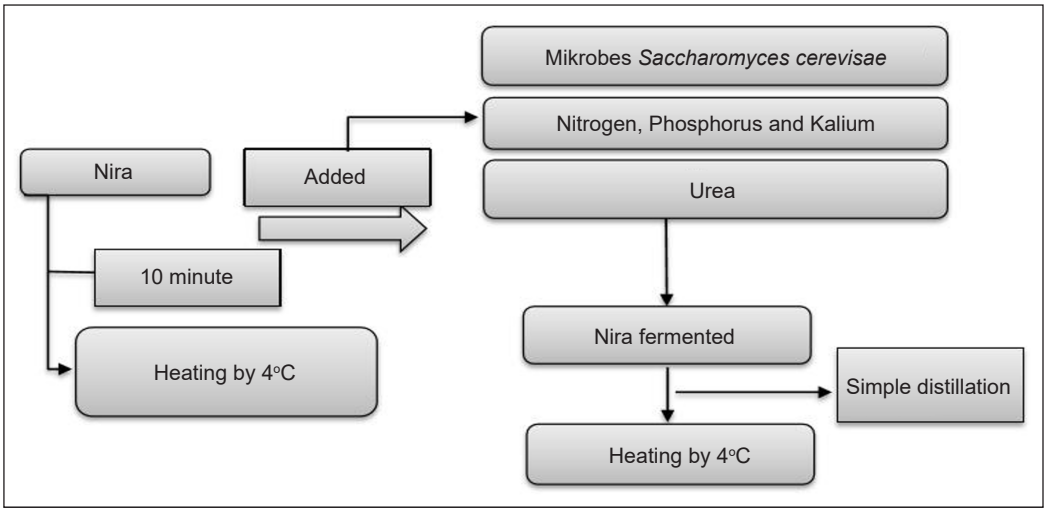

Figure 2. Bioethanol production process

how the initial design was planned for the tool to be made (Sivamani & Baskar, 2018). The specifications for the bioethanol purification tool designed are Double Jacket tubes with a 20-liter capacity and AISI 304 Stainless Steel (Stainless Steel has excellent corrosion resistance, making it suitable for use in environmental conditions containing hazardous chemicals and very high temperatures) (Yu et al., 2017). Meanwhile, the chemical composition of stainless steel 304 can be seen in Table 1.

Table 1
Chemical composition of stainless steel 304 (Fu et al., 2021)

Element	C	Mn	p	S	Si	Cr	Ni	N
Wt%	≤ 0.08	≤ 2.00	≤ 0.045	≤ 0.030	≤ 1.00	18.0-20.0	8.0–11.0	≤ 0.10

The research process requires selecting the appropriate method, collecting data, and processing and analyzing the data so that it becomes a conclusion that gives birth to new ideas. In this study, the research method was carried out experimentally. The experimental method is that the test is carried out by direct observation to identify a cause-and-effect relationship using several treatments. The test scheme can be observed in Figure 3.

The process of purifying bioethanol from sorghum stalks in this study used a device designed as shown in Figure 4. A vacuum distillation system is designed by applying the Bernoulli principle to the ejector so that the device does not use a vacuum pump; therefore, this tool is called the Bernoulli Distillation System (BDS). A double jacket in a reactor combines methods used in separation processes and chemical reactions involving low pressure. Adding a double jacket to the reactor aims to provide better temperature control for the ongoing chemical reactions. This method allows for more efficient separation of

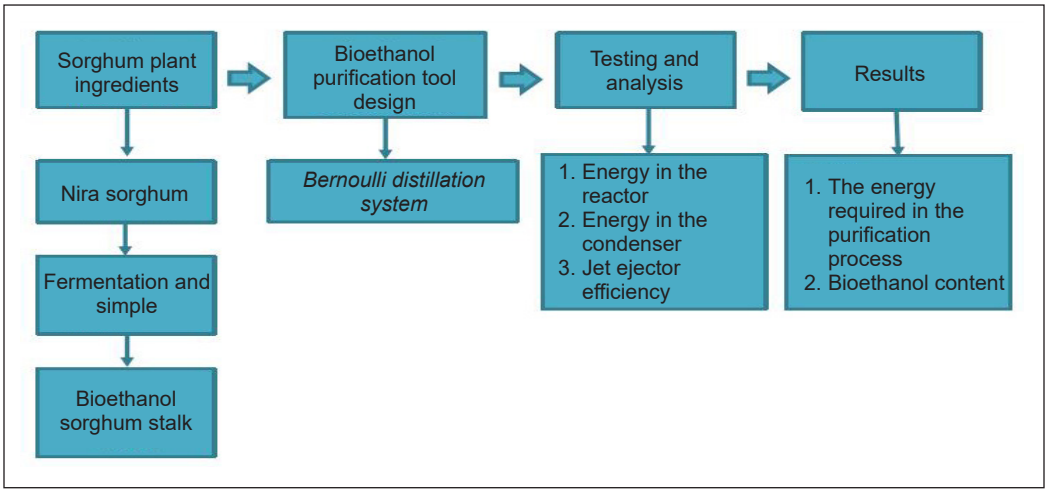

Figure 3. Test scheme

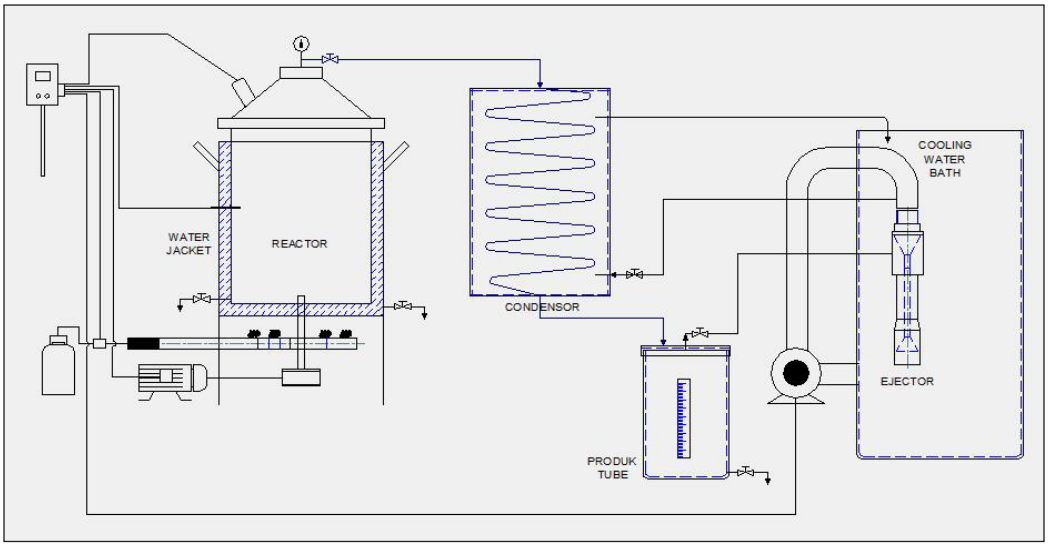

Figure 4. Design of the Bernoulli Distillation System Tool

complex mixtures containing components with significant differences in boiling points. The low pressure created in the vacuum distillation process allows the separation and treatment of the substances at lower temperatures, which can protect components that are sensitive to high temperatures.

The combination of the vacuum distillation method with the ejector and the chemical reaction in the reactor using a double jacket can increase the purity of the product produced. With efficient separation and good temperature control, the desired components can be better separated, and the resulting product can be of higher purity. The use of low pressure in vacuum distillation allows operation at lower temperatures, which reduces energy

requirements for heating. In addition, better temperature control in the reactor can also optimize energy use in chemical reactions.

Primary data from the test results was collected using a data logger. The data logger is a temperature control device with several components, including the Arduino Mega 2560, SD Card, Max 6675 Module, and Type K Thermocouple channel (Spinelli et al., 2019).

RESULTS AND DISCUSSION

Refining bioethanol from sorghum stalks showed maximum results, from 1800 seconds to 7200 seconds. Increased levels of bioethanol indicate that the tool is designed to function properly and efficiently. The material used in the purification process with a content of 28% bioethanol is 20 liters and has increased bioethanol levels as shown in Table 2, where the test for 1800 seconds showed that bioethanol content increased to 48% by 245 ml for 3600 seconds to 51% by 745 ml, for 5400% to 50% as much as 1245 ml, and 7200 seconds to 49% as much as 1645 ml.

Table 2
Heat transfer energy and levels of purified bioethanol

Time Test (second)	Conduction Heat Transfer Energy			Convection Heat Transfer Energy		Produced Bioethanol (ml)	Levels of Purified Bioethanol (%)
	Water Jacket Wall (Joule)	Reactor Tank (Joule)	Reactor Tank Base (Joule)	Reactor Fluid (Joule)	Condenser (Joule)		
1800	-27407.20	663.51	700.70	1.94	33988.50	245	48
3600	-9487.10	962.10	765.05	2.09	66931.20	745	51
5400	8433.00	763.04	722.15	2.00	72683.10	1245	50
7200	14757.72	696.69	707.85	1.96	71637.30	1645	49

Heat Transfer Energy in Reactor

The results of the tests that have been carried out produce data on the values of the wall thermal resistance, the outer wall temperature value, and the inner wall temperature value of the water jacket, reactor tank, and reactor tank bottom. The resulting values are used to obtain conduction heat transfer energy values for the water jacket walls, reactor walls, and reactor wall base, carried out in 1800, 3600, 5400, and 7200 seconds.

Conduction Heat Transfer on the Water Jacket Wall: It is known that the highest temperature on the outer wall is 72°C at 5400 seconds, the highest temperature on the inner wall is 75.25°C at 7200 seconds, and the highest value of conduction heat transfer energy occurred at 7200 seconds with a value of 14757.72 J.

The highest temperature of conduction heat transfer in the reactor tank is known: the outer wall's highest temperature is 81.25°C, the inner wall's highest temperature is

81.04°C at 7200 seconds, and the highest conduction heat transfer energy value occurs at 3600 seconds, rated at 962.1 J.

The highest temperature on the outer wall is 77.98°C, and the highest on the inner wall is 76.97°C at 5400 seconds. The highest conduction heat transfer energy value occurs at 3600 seconds with a value of 765.05 J.

Figure 5 shows the conduction heat transfer on the water jacket wall; the outer wall temperature is 59°C, and the inner wall temperature is 52.5°C at 1800 seconds. From the calculation results, the energy value is (-27407.2) J. The same thing also occurs in the 3600-second conduction heat transfer, which produces an energy value of (-9487.1) J. In the heat transfer test on the energy-water jacket, a negative value means energy loss during the heat transfer (energy losses). The causes of negative energy can involve several factors, including heat radiation, unwanted thermal conduction, and inefficient convection (Vrugt, 2021).

At 5400 and 7200 seconds, the energy values resulting from the calculations show positive values, namely 5400 seconds of 8433 J and 7200 seconds of 14757.72 J. It indicates an energy or energy receipt increase during the heat transfer process. Factors for increasing energy include the addition of external energy and higher heat transfer efficiency (Bezaatpour & Rostamzadeh, 2020).

Figure 6, conduction heat transfer in the reactor tank, shows that the temperature of the reactor tank's outer wall and inner wall from 1800 seconds to 7200 seconds has almost the same increase. The temperature change that occurs at the same time between the outer wall and the inner wall is very small. Some things cause small changes in temperature, including:

1. Wall thickness

   The thicker the wall, the greater the distance heat must travel and the smaller the temperature change. With thinner walls, the temperature change between the outer and inner walls will be more significant (Rakvin et al., 2014).

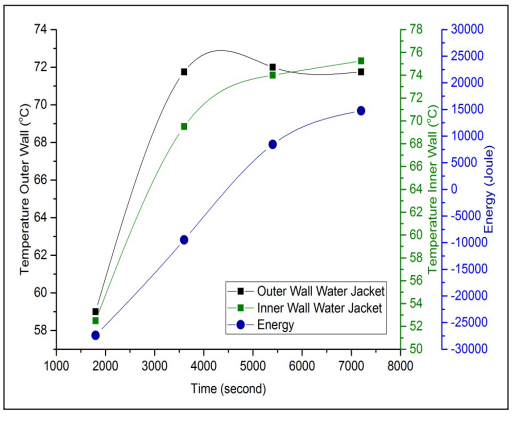

Figure 5. Conduction heat transfer on the water jacket wall

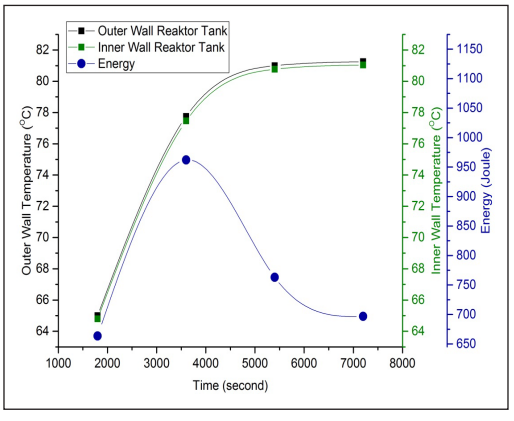

Figure 6. Conduction heat transfer in reactor tanks

2. Initial temperature difference

The initial temperature difference between the outer and inner walls of the reactor tank will also affect the temperature changes that occur in conduction heat transfer. If the initial temperature is close to equilibrium, the temperature change between the outer and inner walls will be very small.

3. Heat transfer coefficient

The heat transfer coefficient is a measure of the efficiency of heat transfer between two surfaces. The higher the heat transfer coefficient, the faster heat can be conducted and the smaller the temperature change. Factors such as surface conditions, fluid flow around the surface, and the fluid's thermal conductivity can affect the heat transfer coefficient (Dongliang et al., 2023).

Meanwhile, the energy generated from the calculation process is known to increase from 1800 to 3600 seconds by 298.59 J. The increase in energy is due to the difference in temperature between two objects that are interconnected. Suppose there is an increase in one of the objects. In that case, heat energy will flow from the object with a higher temperature to the object with a lower temperature, causing an increase in energy for the cooler object (Hu et al., 2023). Furthermore, at 5400 seconds, the energy decreased by 199.06 J; at 7200 seconds, the energy also decreased due to the shrinking temperature difference. The temperature difference between these objects is smaller, so the transfer of heat energy by conduction will be slower, and the energy transferred will be reduced.

Figure 7 shows the conduction heat transfer process on the outer wall of the reactor tank base, which shows an increase in temperature from 1800 seconds to 3600 seconds at 11.34°C. At the same time, a temperature rise of 11.25°C also occurred on the inner wall of the reactor tank base. In the next second, the temperature increase is 2.19°C on the outer wall and 2.25°C on the inner wall. However, at 7200 seconds, the temperature of the outer and inner walls decreased. Temperature rises due to temperature differences and materials' thermal conductivity. The increase and decrease in temperature is a form of thermal equilibrium between two objects that experience a difference in temperature (Wang et al., 2023).

From the results of the calculation analysis, it is known that the value of the heat transfer energy conduction at the base of the reactor tank for 1800 seconds is 700.70 J, 3600 seconds is 765.05 J, 5400 seconds is 722.15 J, and 7200 seconds is

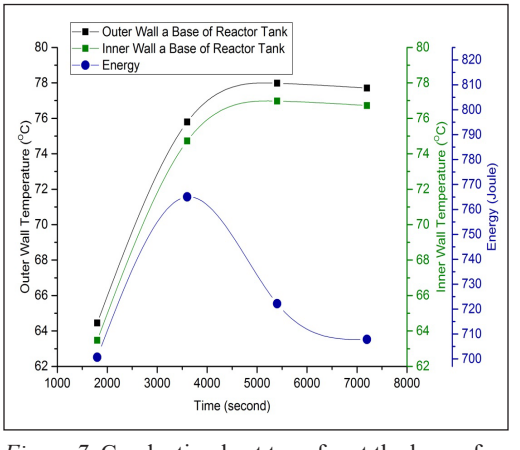

Figure 7. Conduction heat transfer at the base of the reactor tank

707.85 J. At 1800 seconds, 3600 experienced an increase of 64.35 Joules. The increase in energy is caused by a temperature difference between two interconnected objects. Suppose there is an increase in one object. In that case, heat energy will flow from the object with a higher temperature to the object with a lower temperature, causing an increase in energy in the cooler object (Murshed & Castro, 2016). Furthermore, at 5400 seconds and 7200 seconds, the energy produced tends to decrease due to a shrinking temperature difference. The temperature difference between these objects is smaller, so the transfer of heat energy by conduction will be slower, and the energy transferred will be reduced (Ellzey et al., 2019).

The results of the tests that have been carried out produce data on the values of the wall thermal resistance, the reactor wall temperature, and the reactor fluid temperature. The resulting value is used to obtain the energy value of convection heat transfer in the reactor fluid, carried out at 1800, 3600, 5400, and 7200 seconds.

From Table 3, convection heat transfer in the reactor fluid, it is known that the highest temperature on the reactor wall is 76.97°C, the highest temperature in the reactor fluid is 75.74°C at 5400 seconds, and the highest convection heat transfer energy value occurs at 600 seconds with a value of 2.09 J.

Figure 8 shows that the temperature of the inner wall of the reactor increased at 3600 seconds and 5400 seconds and decreased at 7200 seconds. The temperature of the walls in the reactor from 1800 seconds to 3600 seconds increased by 11.25°C; from 3600 seconds to 5400 seconds, it increased by 2.25°C; and from 5400 seconds to 7200 seconds, the temperature dropped by 0.25°C. The temperature rise is due to differences in temperature and materials' thermal conductivity (Anh & Pásztory, 2021). The increase and decrease in temperature is a form of thermal equilibrium between two objects (the outer wall and inner wall) of the reactor tank that experience a temperature difference, which is a conduction heat transfer process (Scotch et al., 2021).

Meanwhile, the temperature of the fluid also increases and decreases, as does the temperature of the reactor wall. The temperature of the reactor fluid from 1800 seconds to 3600 seconds increased by 11.16°C; from 3600 seconds to 5400

Table 3
Convection heat transfer in reactor fluids

Time (second)	Temperature (°C)		Energy (J)
	Reactor Wall	Reactor Fluids	
1800	63.47	62.27	1.94
3600	74.72	73.43	2.09
5400	76.97	75.74	2.00
7200	76.72	75.51	1.96

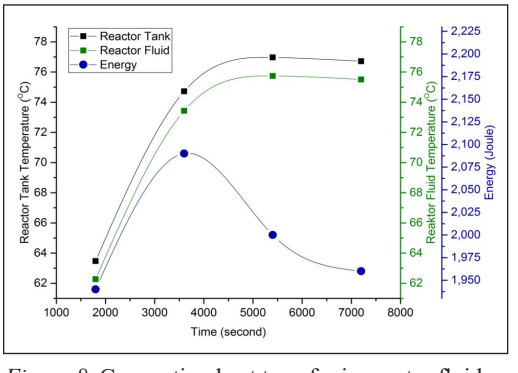

Figure 8. Convection heat transfer in reactor fluids

seconds, it increased by 2.31°C; and from 5400 seconds to 7200 seconds, the temperature decreased by 0.23°C. The temperature increase in the bioethanol fluid can occur due to convection heat transfer from the wall to the reactor fluid. The higher the reactor wall temperature and the higher the temperature difference between the wall and the fluid, the greater the convection heat transfer rate. Reducing the temperature of the reactor wall against the bioethanol fluid can occur by cooling or heat release from the reactor wall to the bioethanol fluid. If the temperature of the reactor wall is higher than the temperature of the bioethanol fluid, heat will flow from the reactor wall to the bioethanol fluid (Morales et al., 2021).

Furthermore, from the results of the calculation of the convection heat transfer energy between the inner wall of the reactor tank and the bioethanol fluid, at 1800 seconds, it was 1.94 Joules. At 3600 seconds, it was 2.09 joules, which experienced an increase in energy of 0.19 Joules. The increase in energy can be affected by temperature differences, as seen in Table 3. Then, at 5400 seconds and 7200 seconds, the energy decreased by 2.00 Joules and 1.96 joules, respectively. Changes in fluid properties can cause energy reduction in convection heat transfer. Fluid properties such as viscosity, thermal conductivity, or density can change with temperature, pressure, or composition changes. This change can affect the efficiency of convection heat transfer so that the energy transferred by convection can be reduced (Yang et al., 2023).

Heat Transfer Energy in the Condenser

The vapor fluid resulting from the distillation process in the reactor tube will then undergo condensation in the condenser tube. This phenomenon is a heat transfer process using the forced convection method (Wang et al., 2022) between the water fluid that touches the condenser pipe wall and bioethanol vapor. Forced convection heat transfer occurs in the condenser at 1800, 3600, 5400, and 7200 seconds.

Table 4 shows the convection heat transfer in the condenser: the highest inlet steam fluid temperature is 60°C, the highest inlet cooling water temperature is 25.25°C, and the highest energy is 72683.1 Joules at 5400 seconds.

Figure 9 shows the temperature of the steam fluid entering the condenser from the test results at 1800 seconds of 41.00°C, 3600 seconds of 55.25°C, 5400 seconds of 60.00°C, and 7200 seconds of 59.00°C. As previously described, the steam fluid obtained from the reactor produces fluids with different temperatures. The temperature

Table 4
Convection heat transfer in condensers

Time (second)	Temperature (°C)		Energy (J)
	Inlet Vapor Fluid	Incoming Cooling Water	
1800	41.00	24.75	33988.5
3600	55.25	23.25	66931.2
5400	60.00	25.25	72683.1
7200	59.00	24.75	71637.3

difference in the vapor fluid is caused by an energy balance process between the reactor's inner wall and the bioethanol fluid in the reactor during the bioethanol purification process.

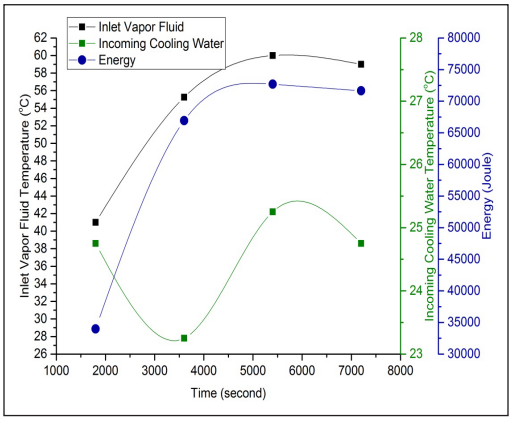

Figure 9. Forced convection heat transfer energy in the condenser

The temperature of the cooling water entering the condenser from the test results at 1800 seconds was 24.75°C, 3600 seconds was 23.25°C, 5400 seconds was 25.25°C, and 7200 seconds was 24.75°C. The temperature of the cooling water entering the condenser increases and decreases due to variations in the cooling load. Changes in the cooling load in the cooling system can cause fluctuations in the cooling water temperature in the condenser. If the cooling load increases, for example, due to an increase in cooling temperature requirements, the cooling water temperature tends to rise because it has to absorb more heat from the condenser. Conversely, the cooling water temperature decreases if the cooling load decreases. Meanwhile, the heat energy in the condenser from the calculation results is known at the 1800th second as 33988.5 Joules, the 3600th second as 66931.2 Joules, the 5400th second as 72683.1 Joules, and the 7200th second as 71637.3 Joules. The energy generated in 1800, 3600, and 5400 seconds has increased, while at 7200 seconds, it has decreased. Variations in the inlet steam temperature affect the increase and decrease in energy. If the temperature of the steam entering the condenser rises, the energy carried by the steam will also increase. It will cause an increase in energy in the condenser. Conversely, if the temperature of the inlet steam drops, the energy carried by the steam will decrease, causing a decrease in energy in the condenser. By using a data logger, it is known that the test results every second for 7200 seconds show that the forced convection heat transfer energy that occurs in the condenser is increasing.

Figure 10 shows the forced convection heat transfer energy in the condenser. Testing for 1800 seconds, the forced convection heat transfer energy at the beginning of the process experienced a decrease in energy from 25000 to 15000 Joules in the 300th second, then experienced an energy increase of 15000 to 42000 Joules in the 1350th second. Likewise, the energy value has increased and decreased in the following seconds, namely for 3600, 5400, and 7200 seconds. Variations influence the increase and decrease in energy in the inlet steam temperature. If the temperature of the steam entering the condenser rises, the energy carried by the steam will also increase. It will cause an increase in energy in the condenser. Conversely, if the temperature of the inlet steam drops, the energy carried by the steam will decrease, causing a decrease in energy in the condenser.

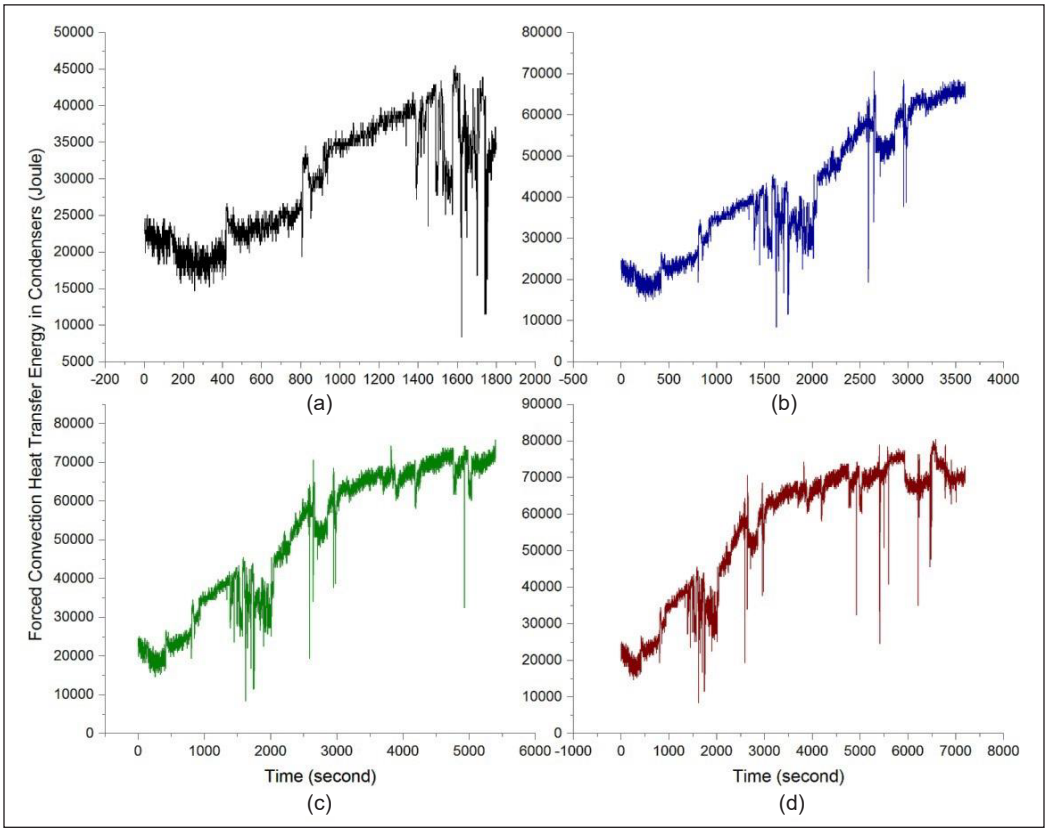

Figure 10. Forced convection heat transfer energy in the condenser: (a) Test for 1800 seconds; (b) Test for 3600 seconds; (c) Test for 5400 seconds; and (d) Test for 7200 seconds

Water Jet Ejector Efficiency

The results of the analysis of the performance of the ejector at a content of 28% bioethanol material show that the Mach Number is the same as 2.75 according to the classification as Compressible Supersonic Flow. In this case, water is included in the supersonic compressible fluid category, which means that it can be compressed and has the ability to flow at speeds that exceed the speed of sound (Dai et al., 2023). In supersonic conditions, the airflow around objects will experience complex changes and cause different aerodynamic effects compared to airflow at subsonic speeds. In supersonic conditions, the air stream is significantly compressed because its pressure increases with speed (Kong & Kim, 2016).

In this case, the water ejector performance efficiency value of 65.4% means that the ejector can produce around 65.4% of the theoretical maximum work that can be achieved under ideal conditions. High-performance efficiency in the water ejector is very important to ensure effective and efficient performance in sucking gas or steam from the surrounding space. The higher the performance efficiency value, the greater the ability of the ejector to

produce maximum and effective work. Several factors affect the performance efficiency of a water ejector, including ejector design, operating fluid pressure, characteristics of the gas or vapor being sucked, and pressure losses in pipes and other components. The performance efficiency of the water jet ejector can produce maximum and effective work in the bioethanol purification process, one of which can be identified by knowing the products produced by the system. After testing the purified bioethanol product, the levels of bioethanol increased.

From Figure 11, it is known that the bioethanol produced always experiences an increase in volume. At 1800 seconds, it was 245 ml; at 3600 seconds, it was 745 ml; at 5400 seconds, it was 1245 ml; and at 7200 seconds, it was 1645 ml. It shows that the bioethanol purification production process went well and efficiently. Meanwhile, the bioethanol content increased from 1800 to 3600 seconds by 48% and 51%, respectively. However, in the next second, the value of the bioethanol content decreased until the end of the purification process.

The increase and decrease in levels of purified bioethanol can be seen from the composition of the raw materials (initial bioethanol) used in the production of bioethanol, which can vary from time to time (Loh et al., 2023). If the raw material composition changes, this can affect the purification process for a predetermined time and temperature and produce different levels of bioethanol. Even though the volume of bioethanol increases, the value of the ethanol content can fluctuate.

Sorghum bioethanol was purified for 2700 seconds, then tested at the Motor Fuel Laboratory, Brawijaya University, Malang, to determine the characteristics of the bioethanol obtained, including the calorific value (cal/gram), viscosity, flash point (°C), and density (g/cm^3).

The resulting calorific value of 1389.48 cal/gram in bioethanol will affect the combustion process and the energy efficiency produced from this fuel (Table 5).

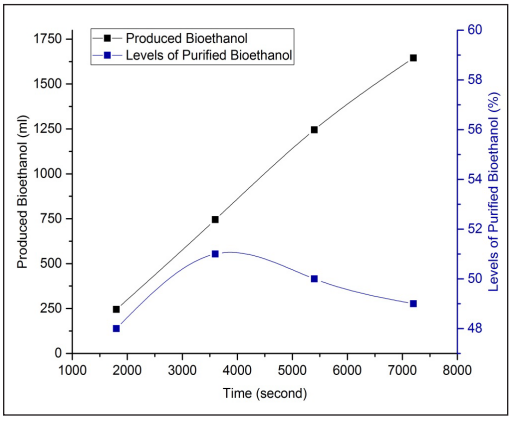

Figure 11. Levels of purified bioethanol

Table 5
Physical properties of bioethanol

No	Standard Bioethanol	Calorific Value (cal/gram)	Viscosity	Flash Point (°C)	Density (g/cm^3)	Reference
1	ASTM D8406	7092.1	1.2–1.5	12	0.7805	Sebayang et al., 2016; Yusuf & Inambao, 2019
2	SNI	6380	1.525	12	0.7890	ESDM RI, 2008
3	Purification Results Bioethanol	1389.48	1.02	32.5	0.9340	This Paper

When bioethanol is burned with oxygen in the combustion process, a chemical reaction produces heat and gases such as carbon dioxide and water vapor. The high calorific value indicates that bioethanol will release more energy per gram during combustion. Bioethanol with a viscosity of 1.02044 shows the level of viscosity of the liquid. The effect of viscosity on the combustion process can affect several aspects, although not as much as the effect of the heating value. The flash point is the minimum temperature at which a fuel, such as bioethanol, will produce enough vapor to form an air-fuel mixture that can temporarily ignite if exposed to flame but does not continue to burn after the flame is removed. In the case of bioethanol, the flash point of 32.5^{o}C indicates that at that temperature, bioethanol will give off steam, which can form a flammable mixture if there is a heat source or fire nearby. Density is a measure of mass per unit volume of a material. Bioethanol with a density of 0.934 g/cm^3 shows a weight of 0.934 grams of bioethanol contained in every cubic centimeter (cm^3) of volume.

CONCLUSION

This research used the Bernoulli Distillation System (BDS) to increase bioethanol levels by analyzing heat transfer energy in the reactor and condenser and the ejector jet's performance efficiency. Based on research results and analysis of heat transfer energy, the Bernoulli Distillation System for 4 times the test time showed an increase in the percentage value of bioethanol content, namely 48%, 51%, 50% and 49%. The highest percentage value of bioethanol content, namely 51%, was obtained in 3600 seconds, the conduction heat transfer energy on the water jacket wall was (-9487.10) J, the reactor tank was 962.10 J, the reactor tank bottom was 765.05 J, the transfer energy the convection heat in the reactor fluid was 2.09 J and the condenser was 66931.20 J. In addition, according to the test results for 2700 seconds, the physical properties of bioethanol were produced, namely a heating value of 1389.48 (cal/gram), viscosity of 1.02, flash point of 32.5 (°C) and density of 0.934 (g/cm^3). Therefore, this bioethanol purification tool is the right tool and has the potential to be developed and further used for other bioethanol purification.

ACKNOWLEDGEMENTS

The authors thank those who have contributed and supported them throughout their journey of completing the study. The authors would also like to extend their gratitude to Universiti Brawijaya, Indonesia, for providing the research facilities.

REFERENCES

Aditiya, H. B., Mahlia, T. M. I., Chong, W. T., Nur, H., & Sebayang, A. H. (2016). Second generation bioethanol production: A critical review. *Renewable and Sustainable Energy Reviews*, *66*, 631–653. https://doi.org/10.1016/j.rser.2016.07.015

Allan, J., Croce, L., Dott, R., Georges, G., & Heer, P. (2022). Calculating the heat loss coefficients for performance modelling of seasonal ice thermal storage. *Journal of Energy Storage*, *52*(PA), Article 104528. https://doi.org/10.1016/j.est.2022.104528

Almeida, L. P., Silva, C. R., Martins, T. B., Pereira, R. D., Esperança, M. N., Cruz, A. J. G., & Badino, A. C. (2021). Heat transfer evaluation for conventional and extractive ethanol fermentations: Saving cooling water. *Journal of Cleaner Production*, *304*, Article 127063. https://doi.org/10.1016/j.jclepro.2021.127063

Amornraksa, S., Subsaipin, I., Simasatitkul, L., & Assabumrungrat, S. (2020). Systematic design of separation process for bioethanol production from corn stover. *BMC Chemical Engineering*, *2*(1), Article 10. https://doi.org/10.1186/s42480-020-00033-1

Anh, L. D. H., & Pásztory, Z. (2021). An overview of factors influencing thermal conductivity of building insulation materials. *Journal of Building Engineering*, *44,* Article 102604. https://doi.org/10.1016/j.jobe.2021.102604

Benedetto, A. D., Sanchirico, R., & Sarli, V. D. (2018). Effect of pressure on the flash point of various fuels and their binary mixtures. *Process Safety and Environmental Protection*, *116*, 615–620. https://doi.org/10.1016/j.psep.2018.03.022

Bezaatpour, M., & Rostamzadeh, H. (2020). Heat transfer enhancement of a fin-and-tube compact heat exchanger by employing magnetite ferrofluid flow and an external magnetic field. *Applied Thermal Engineering*, *164*, Article 114462. https://doi.org/10.1016/j.applthermaleng.2019.114462

Chandan, R. R., Aditya, C. R., Elankeerthana, R., Anitha, K., Sabitha, R., Sathyamurthy, R., Mohanavel, V., & Sudhakar, M. (2022). Machine learning technique for improving the stability of thermal energy storage. *Energy Reports*, *8*, 897–907. https://doi.org/10.1016/j.egyr.2022.09.205

Chen, H., & Fu, X. (2016). Industrial technologies for bioethanol production from lignocellulosic biomass. *Renewable and Sustainable Energy Reviews*, *57*, 468–478. https://doi.org/10.1016/j.rser.2015.12.069

Dai, C., Sun, B., Yue, L., Zhou, S., Zhuo, C., Zhou, C., & Yu, J. (2023). Thermochemical non-equilibrium flow characteristics of high Mach number inlet in a wide operation range. *Chinese Journal of Aeronautics, 36*(12), 164-184. https://doi.org/10.1016/j.cja.2023.07.033

Dongliang, M., Yi, L., Tao, Z., & Yanping, H. (2023). Research on prediction and analysis of supercritical water heat transfer coefficient based on support vector machine. *Nuclear Engineering and Technology, 55*(11), 4102-4111. https://doi.org/10.1016/j.net.2023.07.030

Effendy, M., Yao, Y., & Yao, J. (2013). Effect of mesh topologies on wall heat transfer and pressure loss prediction of a blade coolant passage. *Applied Mechanics and Materials*, *315*, 216–220. https://doi.org/10.4028/www.scientific.net/AMM.315.216

Ellzey, J. L., Belmont, E. L., & Smith, C. H. (2019). Heat recirculating reactors: Fundamental research and applications. *Progress in Energy and Combustion Science*, *72*, 32–58. https://doi.org/10.1016/j.pecs.2018.12.001

ESDM RI. (2008). *Keputusan Direktur Jenderal Minyak dan Gas Bumi* [Decision of the Director General of Oil and Gas]. (Report no. 23204.K/10/DJM.S/2008). Ministry of Energy and Mineral Resources Republic of Indonesia.

Fu, P., Hu, B., Lan, X., Yu, J., & Ye, J. (2021). Simulation and quantitative study of cracks in 304 stainless steel under natural magnetization field. *NDT and E International*, *119*, Article 102419. https://doi.org/10.1016/j.ndteint.2021.102419

Gholinia, M., Pourfallah, M., & Chamani, H. R. (2018). Numerical investigation of heat transfers in the water jacket of heavy duty diesel engine by considering boiling phenomenon. *Case Studies in Thermal Engineering*, *12*, 497–509. https://doi.org/10.1016/j.csite.2018.07.003

Hu, J., Guo, L., Yang, H., He, X., & Luo, Y. (2023). Improvement methods for thermal backflow phenomenon in engine compartment blow-type air cooler module. *Case Studies in Thermal Engineering*, *49*, Article 103182. https://doi.org/10.1016/j.csite.2023.103182

Jiaqiang, E., Zhang, Z., Tu, Z., Zuo, W., Hu, W., Han, D., & Jin, Y. (2018). Effect analysis on flow and boiling heat transfer performance of cooling water-jacket of bearing in the gasoline engine turbocharger. *Applied Thermal Engineering*, *130*, 754–766. https://doi.org/10.1016/j.applthermaleng.2017.11.070

Kartawiria, I. S., Syamsu, K., Noor, E., & Sa'Id, E. G. (2015). Sorghum stalk juice pre-treatment method for bioethanol fermentation process. *Energy Procedia*, *65*, 140–145. https://doi.org/10.1016/j.egypro.2015.01.047

Kong, F., & Kim, H. D. (2016). Optimization study of a two-stage ejector-diffuser system. *International Journal of Heat and Mass Transfer*, *101*, 1151–1162. https://doi.org/10.1016/j.ijheatmasstransfer.2016.05.129

Li, Z., Liang, Z., Wang, C., & Wu, T. (2023). Optimization of heat transfer and temperature control of battery thermal management system based on composite phase change materials. *Surfaces and Interfaces*, *36*, Article 102621. https://doi.org/10.1016/j.surfin.2022.102621

Loh, S. R., Tan, I. S., Foo, H. C. Y., Tan, Y. H., Lam, M. K., & Lim, S. (2023). Exergy analysis of a holistic zero waste macroalgae-based third-generation bioethanol biorefinery approach: Biowaste to bioenergy. *Environmental Technology and Innovation*, *30*, Article 103089. https://doi.org/10.1016/j.eti.2023.103089

Luyben, W. L. (2022). Optimum vacuum distillation pressure. *Chemical Engineering and Processing - Process Intensification*, *171*, Article 108630. https://doi.org/10.1016/j.cep.2021.108630

Malherbe, S. J. M., Cripwell, R. A., Favaro, L., Zyl, W. H. V., & Viljoen-Bloom, M. (2023). Triticale and sorghum as feedstock for bioethanol production via consolidated bioprocessing. *Renewable Energy*, *206*, 498–505. https://doi.org/10.1016/j.renene.2023.02.047

Manente, G., Ding, Y., & Sciacovelli, A. (2022). A structured procedure for the selection of thermal energy storage options for utilization and conversion of industrial waste heat. *Journal of Energy Storage*, *51*, Article 104411. https://doi.org/10.1016/j.est.2022.104411

Morales, M., Arvesen, A., & Cherubini, F. (2021). Integrated process simulation for bioethanol production: Effects of varying lignocellulosic feedstocks on technical performance. *Bioresource Technology*, *328*, Article 124833. https://doi.org/10.1016/j.biortech.2021.124833

Murshed, S. M. S., & Castro, C. A. N. D.(2016). Conduction and convection heat transfer characteristics of ethylene glycol based nanofluids – A review. *Applied Energy*, *184*, 681–695. https://doi.org/10.1016/j.apenergy.2016.11.017

Ndapamuri, M. H., Herawati, M. M., & Meitiniarti, V. I. (2021). Production of sugar from sweet sorghum stems with hydrolysis method using trichoderma viride. *Biosaintifika*, *13*(1), 121–127. https://doi.org/10.15294/biosaintifika.v13i1.25954

Nnaemeka, I. C., Egbuna Samuel, O., Onoh Maxwell, I., Christain, A. O., & Chinelo S, O. (2021). Optimization and kinetic studies for enzymatic hydrolysis and fermentation of colocynthis vulgaris Shrad seeds shell for bioethanol production. *Journal of Bioresources and Bioproducts*, *6*(1), 45–64. https://doi.org/10.1016/j.jobab.2021.02.004

Rakvin, M., Markučic, D., & Hižman, B. (2014). Evaluation of pipe wall thickness based on contrast measurement using Computed Radiography (CR). *Procedia Engineering*, *69*, 1216–1224. https://doi.org/10.1016/j.proeng.2014.03.112

Scotch, C. G., Murgulet, D., & Constantz, J. (2021). Time-series temperature analyses indicate conduction and diffusion are dominant heat-transfer processes in fine sediment, low-flow streams. *Science of the Total Environment*, *768*, Article 144367. https://doi.org/10.1016/j.scitotenv.2020.144367

Sebayang, A. H., Masjuki, H. H., Ong, H. C., Dharma, S., Silitonga, A. S., Mahlia, T. M. I., & Aditiya, H. B. (2016). A perspective on bioethanol production from biomass as alternative fuel for spark ignition engine. *RSC Advances*, *6*(18), 14964–14992. https://doi.org/10.1039/c5ra24983j

Sippola, H., & Taskinen, P. (2018). Activity of supercooled water on the ice curve and other thermodynamic properties of liquid water up to the boiling point at standard pressure. *Journal of Chemical and Engineering Data*, *63*(8), 2986–2998. https://doi.org/10.1021/acs.jced.8b00251

Sivamani, S., & Baskar, R. (2018). Process design and optimization of bioethanol production from cassava bagasse using statistical design and genetic algorithm. *Preparative Biochemistry and Biotechnology*, *48*(9), 834–841. https://doi.org/10.1080/10826068.2018.1514512

Spinelli, G. M., Gottesman, Z. L., & Deenik, J. (2019). A low-cost arduino-based datalogger with cellular modem and FTP communication for irrigation water use monitoring to enable access to CropManage. *HardwareX*, *6*, Article e00066. https://doi.org/10.1016/j.ohx.2019.e00066

Suryaningsih, R., & Irhas. (2014). Bioenergy plants in indonesia: Sorghum for producing bioethanol as an alternative energy substitute of fossil fuels. *Energy Procedia*, *47*, 211–216. https://doi.org/10.1016/j.egypro.2014.01.216

Vrugt, M. T. (2021). The mereology of thermodynamic equilibrium. *Synthese*, *199*(5–6), 12891–12921. https://doi.org/10.1007/s11229-021-03359-2

Wang, C. H., Liu, Z. Y., Jiang, Z. Y., & Zhang, X. X. (2022). Numerical investigations of convection heat transfer in a thermal source-embedded porous medium via a lattice Boltzmann method. *Case Studies in Thermal Engineering*, *30*, Article 101758. https://doi.org/10.1016/j.csite.2022.101758

Wang, M., Bu, S., Zhou, B., Li, Z., & Chen, D. (2023). Multi-scale heat conduction models with improved equivalent thermal conductivity of TRISO fuel particles for FCM fuel. *Nuclear Engineering and Technology*, *55*(3), 1140–1151. https://doi.org/10.1016/j.net.2022.12.001

Xiao, R., Zhang, Y., Chen, L., Wang, J., Chen, S., & Hou, Y. (2023). Effects of circumferential heat conduction on heat transfer characteristics of supercritical R134a in horizontal tubes. *International Journal of Thermal Sciences*, *183*, Article 107884. https://doi.org/10.1016/j.ijthermalsci.2022.107884

Yang, Y., AL-Khafaji, M. O., Fazilati, M. A., Hassan Saeed, S., Salman, N. A., Abdulkadhim, A. H., Shaghnab, M. L., Gatea, M. A., Jawad, A. J. M., & Toghraie, D. (2023). Energy and exergy analysis of a liquid desiccant heat and mass transfer loop with natural convection: The effect of heat sink and heat source temperature. *Case Studies in Thermal Engineering*, *45*, Article 102833. https://doi.org/10.1016/j.csite.2023.102833

Yu, J., Ji, G., Liu, Q., Zhang, J., & Shi, Z. (2017). Effect of sol-gel ZrO2 films on corrosion behavior of the 304 stainless steel in coal-gases environment at high temperature. *Surface and Coatings Technology*, *331*, 21–26. https://doi.org/10.1016/j.surfcoat.2017.10.037

Yusuf, A. A., & Inambao, F. L. (2019). Bioethanol production from different Matooke peels species: A surprising source for alternative fuel. *Case Studies in Thermal Engineering*, *13*, Article 100357. https://doi.org/10.1016/j.csite.2018.11.008

Zabed, H., Sahu, J. N., Suely, A., Boyce, A. N., & Faruq, G. (2017). Bioethanol production from renewable sources: Current perspectives and technological progress. *Renewable and Sustainable Energy Reviews*, *71*, 475–501. https://doi.org/10.1016/j.rser.2016.12.076